Isotopic Mapping of Transition-State Structural Features Associated with Enzymic Catalysis of Methyl Transfer[1]

James Rodgers, Douglas A. Femec, and Richard L. Schowen*

Contribution from the Department of Chemistry, University of Kansas, Lawrence, Kansas 66045.
Received April 27, 1981

Abstract: For comparison of the molecular structures of nonenzymic and enzymic sulfur-to-oxygen transmethylation transition states by the use of kinetic isotope effects a series of isotopic maps is produced. In these, contours of constant isotope effect are displayed vs. the Pauling bond orders B_{CS} and B_{CO}, for the carbon–sulfur and carbon–oxygen bonds, respectively, taken as independent variables to describe the transition states. Maps are calculated by the BEBOVIB approach for $k(CH_3)/k(CD_3)$, $k(^{12}CH_3)/k(^{13}CH_3)$, $k(^{16}O)/k(^{18}O)$, and $k(^{32}S)/k(^{34}S)$, with two models for the reaction coordinate, two force-field assumptions, and four temperatures. Nonenzymic isotope effects and isotope effects for catechol-*O*-methyltransferase action are then used to construct figures on the CH_3/CD_3 and $^{12}CH_3/^{13}CH_3$ maps which correspond to "allowed" spaces of transition-states structures. Superposition of the figures yields the spaces of transition-state structures simultaneously consistent with both hydrogen and carbon isotope effects. It is concluded that the enzyme compresses the S_N2 transition state and that the compression of the C–O and C–S bonds may well be of the order of 0.15 Å per bond and could conceivably be more than twice as large.

The enzymic methylation of a large number of different nucleophiles by *S*-adenosylmethionine (AdoMet, **1**, Figure 1) is a critical event for many biological phenomena, including information storage and retrieval in bacteria, neurosecretory processes in the brain, the processing of nucleic acids, hormone inactivation, detoxification of exogeneous compounds, and the metabolism of drugs.[2] The reaction (eq 1; AdoHcy is *S*-adenosylhomocysteine)

$$\underset{\mathbf{1}}{\text{Nu: + CH}_3\text{–AdoHcy}^+ (\equiv\text{AdoMet})} \xrightarrow{[\text{Nu–CH}_3\text{–AdoHcy}]} \text{Nu–CH}_3^+ + \text{AdoHcy} \quad (1)$$

occurs through an S_N2-like transition state,[3,4] and α-deuterium isotope effects for the enzymic reaction and related nonenzymic reactions suggest that the enzymic reaction has an unusually "tight" transition state (short sulfur-to-nucleophile distance)[4-6] in the case of catechol-*O*-methyltransferase (COMT).

We present here a method of using model vibrational analysis calculations[7,8] to generate semiquantitative, relative structural information about a series of transition states for sulfur-to-oxygen transmethylation and transalkylation, including the transition state for COMT action. The concept involves the generation of maps of isotope-effect predictions as a function of transition-state structure, which one hopes will span the space of all reasonable transition-state structures. In the present case, the models for the transition states were variations on the structure of Figure 2. The two Pauling bond orders[9] B_{CO} and B_{CS}, for the forming C–O bond and breaking C–S bond, respectively, were chosen as independent variables. Equation 2 (Pauling's rule) was taken[10]

$$B = \exp[(R_1 - R_B)/0.3] \quad (2)$$

to define these bonds orders in terms of the bond distances R_B (for a bond of order B) and R_1 (for a bond of unit order). Thus, specification of these two bond orders constituted a choice of transition-state structure; all structural features of the transition state and its force field were related to the two bond orders. (For greater generality, several sets of assumptions about the force fields and relationships were used.)

For a particular isotope effect (e.g., $k(CH_3)/k(CD_3)$), the predicted effects as a function of the transition-state structural variables B_{CO} and B_{CS} form a three-dimensional surface; this surface can be projected as a map of contours of constant isotope effect on the B_{CO}, B_{CS} plane. If one has an experimental isotope effect along with some measure of its experimental error (like the standard deviation), a figure can be traced out upon the map, which includes all transition-state structures consistent with the measured isotope effect and values within, say, one or two standard deviations. To the extent that the calculations are reliable, such a figure will contain the space of transition structures "allowed" by the experimental measurement.

Similar maps can then be constructed for other isotope effects—for example, $k(^{12}CH_3)/k(^{13}CH_3)$—and figures can be drawn on these maps, which contain the transition-state structures "allowed" by experimental measurements of these isotope effects. Then the maps of allowed structures can be superimposed and the intersection of all the "allowed" spaces for the various measured isotope effects found. This reduced space then contains the transition-state structures that are *simultaneously* consistent with *all* isotope effects. In fortunate cases, a rather narrow set of structures might emerge from such a procedure.

At the present time, our ignorance of the structural features of transition states[11] and of the details of their force fields[7,8] is too great to permit a highly exacting application of the technique just described. Still, it should lead to a general idea of what transition-state structures are like. Further, when the same set of maps is applied to a series of similar reactions, various errors in structure and force field may have a similar effect along the series. Then the *relative* structural features derived from the treatment may be quite accurate.

This makes an application to enzyme catalysis especially favorable. Here we want to compare enzymic and nonenzymic transition states for the same reaction, in order to see what effect

(1) This research was supported by the National Institutes of Health through Grant No. GM-20199 from the National Institute of General Medical Sciences and by an allocation of computer time from the University of Kansas.
(2) Usdin, E.; Borchardt, R. T.; Creveling, C. R., Eds. "Transmethylation"; Elsevier: North Holland, New York, 1979.
(3) Mascaro, L.; Hörhammer, R.; Eisenstein, S.; Sellers, L. K.; Mascaro, K.; Floss, H. G. *J. Am. Chem. Soc.* **1977**, *99*, 273.
(4) Hegazi, M. F.; Borchardt, R. T.; Schowen, R. L. *J. Am. Chem. Soc.* **1979**, *101*, 4359–4365.
(5) Mihel, I.; Knipe, J. O.; Coward, J. K.; Schowen, R. L. *J. Am. Chem. Soc.* **1979**, *101*, 4349–4351.
(6) Gray, C. H.; Coward, J. K.; Schowen, K. B.; Schowen, R. L. *J. Am. Chem. Soc.* **1979**, *101*, 4351–4358.
(7) Buddenbaum, W. E.; Shiner, V. J., Jr. In "Isotope Effects on Enzyme-Catalyzed Reactions"; Cleland, W. W., O'Leary, M. H., Northrop, D. R., Eds.; University Park Press: Baltimore, MD, 1977.
(8) Melander, L.; Saunders, W. H., Jr. "Reaction Rates of Isotopic Molecules"; Wiley: New York, 1980.
(9) Pauling, L. "The Nature of the Chemical Bond", 3rd ed.; Cornell University Press: Ithaca, NY, 1960; p 239.
(10) Burton, G. W.; Sims, L. B.; Wilson, J. C.; Fry, A. *J. Am. Chem. Soc.* **1977**, *99*, 3371.
(11) Gandour, R. D.; Schowen, R. L., Eds. "Transition States of Biochemical Processes"; Plenum Press: New York, 1978.

0002-7863/82/1504-3263$01.25/0

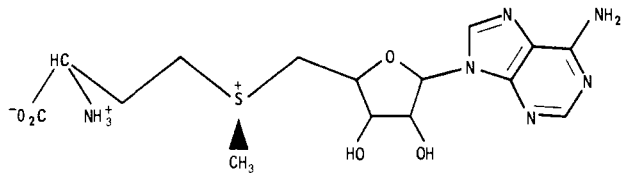

Figure 1. *S*-Adenosylmethionine (AdoMet, **1**), which serves widely as a biological methyl donor. This approximately scaled projection emphasizes the bilaterally alate structure of the leaving-group sulfide AdoHcy, with its zwitterionic wing extending to the left and its highly functionalized adenosyl wing extending to the right.

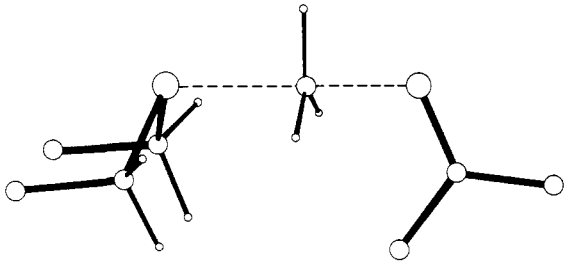

Figure 2. Model used for transmethylation transition state, reactants, and products. The structure is drawn for a transition state in which both partial bonds (dashed lines; C--S to the left, C--O to the right) have Pauling bond orders B_{CS} and B_{CO} of 0.5. The methyl group is therefore planar, in the central part of the structure. The seven-atom fragment at left, $(CCH_2)_2S$, represents the sulfide leaving group of a sulfonium methyl donor. The four-atom fragment at right, C_3O, represents the catecholic methyl acceptor of the COMT reaction.

the enzyme has had. In this paper, then, we generate such maps for S-to-O methyl transfer and compare allowed transition-state structures for nonenzymic and enzymic reactions.

Experimental Section

Method of Calculation. The program written by Sims and his coworkers,[10] known as BEBOVIB-IV, was used in the form available from the Quantum Chemistry Program Exchange. Calculations were carried out on the Honeywell 66/60 computer in the Academic Computer Center of the University of Kansas.

Principal Reaction Variables. Two independent variables, the Pauling bond orders B_{CS} of the breaking C–S bond and B_{CO} of the forming C–O bond, were employed and were allowed to vary between zero and unity. These variables were used to generate transition-state geometrical structures and force fields from data on stable molecules.

Reactant and Product Models. Geometrical parameters employed for the reactant models **2** and **3** (representing AdoMet, **1**, and a catecholic

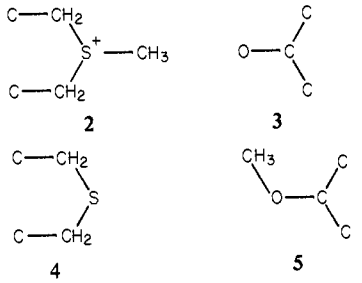

methyl acceptor; see Figure 2), and the product models **4** and **5** (representing AdoHcy and the methylated catechol) are given in Table I. Most were derived from standard tabulations[12] or from structural studies of sulfur compounds[13-19] or dimethyl ether.[20] The data are shown as features particular to the "$(CCH_2)_2S$ fragment" (i.e., **4**), the "C_3O fragment" (**3**), and the "CH_3 fragment". Under the last are tabulated, in addition to characteristics of the CH_3 group itself, those features added by its presence in **2** and **5**.

Force constants for reactant and product molecules are given in Table II. Those for the reactant model **2** were taken from the compilation for

Table I. Geometrical Parameters for Reactant and Product Models

parameter[a]	reactant value	product value
	$(CCH_2)_2S$ Fragment	
C-C	1.54	1.54
C-S	1.81	1.81
C-H	1.11	1.11
C-C-S	109.5	109.5
C-C-H	109.5	109.5
H-C-H	109.5	109.5
C-S-C	102.1	102.1
C-C-S-C	74.6	74.6
C-S-C-C	74.6	74.6
	CH_3 Fragment[b]	
C_M-H	1.11	1.11
H-C_M-H	109.5	109.5
C_M-S	1.81	
H-C_M-S	109.5	
C_M-S-C	102.1	
(H-C_M-S-C)[c]	127.3	
C_M-S-C-C	180.0	
C_M-O		1.41
H-C_M-O		109.5
C_M-O-C		111.7
H-C_M-S-C[c]		180.0
C_M-O-C-C[d]		0.0
	C_3O Fragment[e]	
C-O	1.34	1.34
C-C	1.39	1.39
O-C-C	120.0	120.0
C-C-C	120.0	120.0

[a] Parameters designated by two atoms are bond lengths (A), by three atoms are bond angles (deg), and by four atoms are dihedral angles (deg). [b] C_M designates the carbon of the methyl group. [c] The H-C_M bond here is the "vertical" HC bond, lying in the plane of Figure 2. [d] This dihedral angle is for the "endo" C-C bond of the C_3O fragment. [e] Planar.

Table II. Force Constants for Reactant and Product Models[a,b]

internal coordinate	reactant	product
	$(CCH_2)_2S$ Fragment	
C-C	4.50	4.50
C-S	3.20	3.25
C-H	4.70	4.70
C-C-S	1.00	0.85
C-C-H	0.67	0.67
H-C-H	0.54	0.54
C-S-C	1.50	1.50
	CH_3 Fragment[c]	
C_M-H	4.70	4.70
H-C_M-H	(0.52)[d]	(0.52)[e]
C_M-S	3.20	
H-C_M-S	0.62	
C_M-S-C	1.50	
C_M-O		5.10
H-C_M-O		0.88
C_M-O-C		1.50
	C_3O Fragment	
C-O	7.00	5.40
C-C	7.60	7.60
O-C-C	0.85	1.30
C-C-C	1.00	1.00
out-of-plane	0.50	0.50

[a] Stretching force constants are in mdyn/A and bending force constants are in mdyn·A/rad². [b] All torsional force constants were assigned a value of 0.03 mdyn·A/rad². [c] C_M designates the carbon of the methyl group. [d] Value for set no. 2; 0.54 for set no. 1. [e] Value for set no. 2; 0.50 for set no. 1.

(12) March, J. "Advanced Organic Chemistry: Reactions, Mechanisms, Structure"; McGraw-Hill: New York, 1968; pp 22, 31.
(13) Barnes, W.; Sundaralingam, M. *Acta Crystallogr., Sect. B* **1973**, *B29*, 1868.
(14) Kilbourn, T.; Felix, D. *J. Chem. Soc. A* **1969**, 163.
(15) Zimmermann, I. C.; Barlow, N.; McCullough, J. D. *Acta Crystallogr.* **1963**, *16*, 883.
(16) Guy, J. J.; Hamor, T. A. *J. Chem. Soc., Perkin Trans. 2* 1975, 467.
(17) Zuccaro, D. E.; McCullough, J. D. *Z. Kristallogr.* **1959**, *112*, 401.
(18) Lopez-Castro, A.; Truter, M. R. *Acta Crystallogr.* **1964**, *17*, 465.
(19) Fenn, R. H. *Acta Crystallogr.* **1966**, *20*, 20.
(20) Blukis, U.; Kasai, P. H.; Myers, R. J. *J. Chem. Phys.* **1963**, *38*, 2753.

a number of typical sulfur compounds, made by Scott and El-Sabban.[21] They were rounded to the nearest 0.1 mdyn/Å (for stretches) or the nearest 0.01 mdyn·Å/rad² (for bends) except for the methyl H–C–H bending force constants. These were in one case ("set no. 1") fixed at 0.54 mdyn·Å/rad² (from Scott and El-Sabban[21]) in **2** and allowed to decrease to 0.50 mdyn·Å/rad² in **5** (from a study of esters by Boeri and Bahl[23]). In a second case ("set no. 2"), they were set at 0.52 mdyn·Å/rad² throughout. Except for these constants and the C–S stretching force constant, all force constants for the $(CCH_2)_2S$ fragment were made the same in the product **4** as in the reactant **2**. The C–S stretching constants were allowed to rise to 3.25 mdyn/Å from 3.20 mdyn/Å to simulate the expected increase upon loss of the positive charge at sulfur.

The force constants for the methyl-acceptor model **3** and the corresponding product **5** were derived from standard sources[22] and from the studies of ethers by Snyder and Zerbi[24] and of aromatic acid esters by Boeri and Bahl.[23] The C–C–C and out-of-plane constants are from the latter[23] and were used for both **3** and **5**. The O–C–C constant for the reactant was taken as that for a typical sp^2 substituent on a phenyl ring[24] in **3** but was increased in **5** to the value[10] for a typical ether.[23] The C–O stretching constant in the phenoxide model **3** was considered to be that for a C–O bond of order 1.25 and was thus assigned an approximate value between 12 mdyn/Å (for a bond of order two)[22] and 5.4 mdyn/Å (for a bond of order one).[22] The latter was employed for **5**. Force constants associated with the presence of the methyl group in **5** were those for the C_M–O stretch and H–C_M–O bend, both taken from Snyder and Zerbi,[24] and for the C_M–O–C bend, which was averaged between the ether value[24] and a value for a methyl ester.[23]

Transition-State Models. The method for construction of models for transition states with any arbitrary combination of B_{CO} and B_{CS} can be understood in terms of the quantity P, defined by eq 3, which measures the *degree of product character* of a transition state.

$$P = B_{CO}/(B_{CO} + B_{CS}) \tag{3}$$

All geometrical features of the $(CCH_2)_2S$ fragment and the C_3O fragment were taken not to vary between reactant and product; these features were therefore kept constant at the values of Table I for all transition states. The lengths of the C–H bonds of the transferring methyl group were also constant.

The lengths of the C_M–O and C_M–S bonds were calculated from their bond orders according to eq 2 and their force constants from eq 4, where

$$F_B = BF_1 \tag{4}$$

F_B is the stretching force constant for a bond of order B, and F_1 for a bond of unit order. The H–C_M–S and H–C_M–O angles for the transferring methyl group were so chosen as to generate Walden inversion; they are thus given by eq 5 (P from eq 3). The H–C_M–H and other

$$\theta(\text{H–C}_M\text{–S, deg}) = 70.5 + (39.0)(1 - P) \tag{5a}$$

$$\theta(\text{H–C}_M\text{–O, deg}) = 70.5 + 39.0P \tag{5b}$$

angles were automatically fixed by these rules and the assumption of exactly collinear methyl transfer.

The force constants for the $(CCH_2)_2S$ and C_3O fragments were varied smoothly between reactant and product values as shown in eq 6a and 6b, respectively. The bending force constants associated with the presence

$$F(B_{CS}) = B_{CS}F(\text{reactant}) + (1 - B_{CS})F(\text{product}) \tag{6a}$$

$$F(B_{CO}) = (1 - B_{CO})F(\text{reactant}) + B_{CO}F(\text{product}) \tag{6b}$$

of the methyl group in **2** and **5** (for angles H–C_M–S, C_M–S–C and angles H–C_M–O and C_M–O–C, respectively) were varied according to eq 7a and 7b.

$$F(B_{CS}) = B_{CS}F(\text{reactant}) \tag{7a}$$

$$F(B_{CO}) = B_{CO}F(\text{product}) \tag{7b}$$

Two different protocols were employed for fixing the force constants for the C_M–H stretch and the H–C_M–H bends, directly associated with the transferring methyl group.

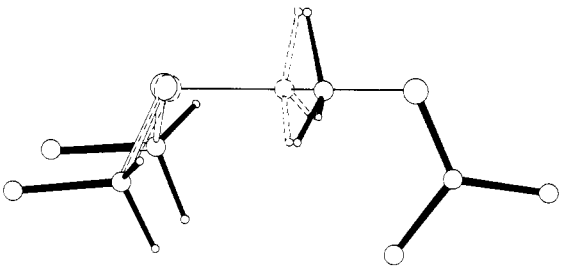

Figure 3. Reaction-coordinate motion according to eq 11. The atoms (the same as in Figure 2) are shown at their extreme amplitudes of extension and compression in the eigenvector corresponding to the imaginary frequency when both B_{CO} and B_{CS} are 0.5. Amplitudes less than about 15% of the amplitude for the methyl carbon are not explicitly shown, although no atom has a zero amplitude in this motion.

Set no. 1: The magnitudes of both the C–H stretching and HCH bending constants were maximized for the half-transferred methyl group (eq 8 and 9, respectively).

$$F(P)\ (\text{mdyn/Å}) = 4.70 + 0.60P\ (P \le 0.5) \tag{8a}$$

$$F(P)\ (\text{mdyn/Å}) = 4.70 + 0.60(1 - P)\ (P \ge 0.5) \tag{8b}$$

$$F(P)\ (\text{mdyn·Å/rad}^2) = 0.54 + 0.12P\ (P \le 0.5) \tag{9a}$$

$$F(P)\ (\text{mdyn·Å/rad}^2) = 0.50 + 0.20(1 - P)\ (P \ge 0.5) \tag{9b}$$

Set no. 2: The magnitude of the C–H stretching force constant was held at 4.70 mdyn/Å and the H–C–H bending force constant at 0.52 mdyn·Å/rad² for all transition states.

Reaction-Coordinate Generation. In the customary way,[8] the model was caused to simulate an activated complex through use of off-diagonal force-constant matrix elements to generate an imaginary reaction-coordinate frequency. In the simplest scheme, the stretching coordinate for the breaking C–S bond (force constant F_{CS}) was coupled to the stretching coordinate for the forming C–O bond (force constant F_{CO}) according to eq 10. The form of the resulting normal coordinate is far from ideal:

$$F_{CS,CO} = 1.1(F_{CS}F_{CO})^{1/2} \tag{10}$$

the CH_3 group moves as a unit, with no inclusion of the inverting motion that one naturally associates with an S_N2 reaction.[7] A second scheme was therefore used to generate a more natural form: the HCS and HOC bending coordinates were coupled into the reaction coordinate by adding the conditions of eq 11 to that of eq 10. The result of this "bend–stretch

$$F_{HCS,CS} = 0.1F_{CS,CO} \tag{11a}$$

$$F_{HCS,CO} = -0.1F_{CS,CO} \tag{11b}$$

$$F_{HCO,CO} = 0.1F_{CS,CO} \tag{11c}$$

$$F_{HCO,CS} = -0.1F_{CS,CO} \tag{11d}$$

coupling" scheme is a reaction coordinate that has the form exemplified in Figure 3. The reaction coordinate generated by eq 10 alone will be referred to hereafter as the "rigid-methyl reaction coordinate", while that produced by the combination of eq 10 and 11 will be denoted the "Walden-inversion reaction coordinate". The absolute magnitudes of the (imaginary) reaction-coordinate frequencies generated in these calculations were less than a few hundred cm^{-1}. The introduction of "bend-stretch coupling" as above, without adjustment of other force constants, has the effect of increasing the absolute magnitude of the imaginary frequency. The magnitudes of other, real frequencies are also changed. The changes are not extremely large for values of coupling constants produced by eq 11, however, and the imaginary-frequency magnitudes remained in the range of hundreds of cm^{-1}. This point was not systematically explored in the present calculations, although we hope to do so in the future.

Results

By the procedures just described, four kinds of isotope effects were calculated: (1) $k(CH_3)/k(CD_3)$ for hydrogen isotopic substitution at the transferring methyl; (2) $k(^{12}CH_3)/k(^{13}CH_3)$ for carbon isotopic substitution at the transferring methyl; (3) $k(^{16}O)/k(^{18}O)$ for oxygen isotopic substitution at the nucleophilic position; (4) $k(^{32}S)/k(^{34}S)$ for sulfur isotopic substitution at the nucleofugic position. Each of these was calculated for 43 combinations of B_{CO} and B_{CS} for two different sets of transition-state force constants ("set no. 1" and "set no. 2" above), for two different

(21) Scott, D. W.; El-Sabban, M. Z. *J. Mol. Spectr.* **1969**, *30*, 317–337.
(22) Wilson, E. B.; Decius, J. C.; Cross, P. C. "Molecular Vibrations"; McGraw-Hill: New York, 1955; p 175.
(23) Boeri, F. J.; Bahl, S. K. *Spectrochim. Acta* **1976**, *32*, 987–1006.
(24) Snyder, R. G.; Zerbi, G. *Spectrochim. Acta, Part A* **1967**, *23A*, 391.

Table III. Contributions to Calculated Kinetic Isotope Effects[a] at 298 K

type of isotope effect[b]	(B_{CS}, B_{CO})[c]	ν/ν'	MMI	EXC^{-1}	ZPE	(k_{light}/k_{heavy})[d]
CD_3, set no. 1[e]	0.9, 0.1	1.0220	1.1050	1.0186	0.8381	0.9092
	0.1, 0.1	1.0037	1.1048	1.3512	1.9071	1.5593
	0.5, 0.5	1.0032	1.1039	0.9836	0.5658	0.6350
	0.9, 0.9	1.0030	1.1035	0.9211	0.2681	0.3212
	0.1, 0.9	1.0245	1.1051	1.0306	0.7185	0.7704
CD_3, set no. 2[e]	0.9, 0.1	1.0216	1.1050	1.0206	0.9254	1.0020
	0.1, 0.1	1.0037	1.1048	1.3545	2.6278	2.1434
	0.5, 0.5	1.0032	1.1039	0.9863	0.7801	0.8731
	0.9, 0.9	1.0030	1.1035	0.9239	0.3699	0.4418
	0.1, 0.9	1.0245	1.1051	1.0306	0.7449	0.7987
$^{13}CH_3$, set no. 1[e]	0.9, 0.1	1.0187	1.0248	1.0173	1.0388	1.0465
	0.1, 0.1	1.0344	1.0245	1.0278	1.0866	1.0831
	0.5, 0.5	1.0341	1.0244	1.0108	1.0566	1.0708
	0.9, 0.9	1.0339	1.0243	1.0025	1.0339	1.0564
	0.1, 0.9	1.0140	1.0238	1.1074	1.0176	1.0240
$^{13}CH_3$, set no. 2[e]	0.9, 0.1	1.0188	1.0248	1.0173	1.0403	1.0480
	0.1, 0.1	1.0344	1.0245	1.0278	1.0910	1.0875
	0.5, 0.5	1.0341	1.0244	1.0108	1.0608	1.0751
	0.9, 0.9	1.0339	1.0243	1.0025	1.0380	1.0605
	0.1, 0.9	1.0140	1.0238	1.0174	1.0179	1.0243
^{18}O[f]	0.9, 0.1	1.0197	1.0786	1.0412	0.9766	1.0117
	0.1, 0.1	1.0090	1.0778	1.0535	0.9711	0.9935
	0.5, 0.5	1.0011	1.0797	1.0370	0.9294	0.9676
	0.9, 0.9	1.0013	1.0805	1.0302	0.9003	0.9443
	0.1, 0.9	1.0063	1.0795	1.0322	0.9086	0.9502
^{34}S[f]	0.9, 0.1	1.0005	1.0085	1.0052	0.9981	1.0014
	0.1, 0.1	1.0031	1.0079	1.0130	1.0215	1.0164
	0.5, 0.5	1.0037	1.0085	1.0066	1.0082	1.0101
	0.9, 0.9	1.0040	1.0088	1.0038	0.9988	1.0038
	0.1, 0.9	1.0101	1.0082	1.0093	1.0248	1.0237

[a] Reaction coordinate with coupling of bends as in Figure 3. [b] See text for sites and character of isotopic substitution. [c] Pauling bond orders of C-S and C-O bonds, respectively. [d] $(k_{light}/k_{heavy}) = (MMI)(EXC)(ZPE)$. [e] See text for definition of force-constant sets. [f] Oxygen and sulfur isotope effects are insensitive to force-constant set choice at this level of precision.

assumptions about reaction-coordinate design (C–O, C–S coupling only, and with inclusion of bends as in Figure 3), and for four different temperatures (273 K, 298 K, 310 K, and 323 K). This amounts to vibrational analysis of 688 transition-state models to produce 2752 isotope effects.

For a given type of isotope effect, temperature, and assumed model, the predictions can be presented as points or contours of constant isotope effect in the $\{B_{CO}, B_{CS}\}$ plane (an "isotopic map"). This work generated 64 such maps.[25] Contours of constant isotope effect were generated by interpolation among the 43 calculated points, and the maps were plotted by using the Surface II Graphics System of the Kansas Geological Survey.[26]

Figure 4 shows typical maps, for what is probably the most realistic set of assumptions, and for 310 K, the temperature at or near which our experiments were for the most part performed.[4-6] Figure 5 shows maps for other sets of assumptions, so that the effect of the assumptions on the results may be appreciated.

Each calculated isotope effect may also be considered[7,8] in terms of its contributions from mass-moment-of-inertia (MMI) changes, changes in populations of excited vibrational states (EXC), and changes in zero-point energy (ZPE). Another factor of interest is ν/ν', the isotopic ratio of reaction-coordinate frequencies. All of these are shown for some typical results in Table III (EXC^{-1} is shown for comparison with MMI; when the product (MMI)(EXC) is unity, the isotope effect arises purely from the ZPE term).

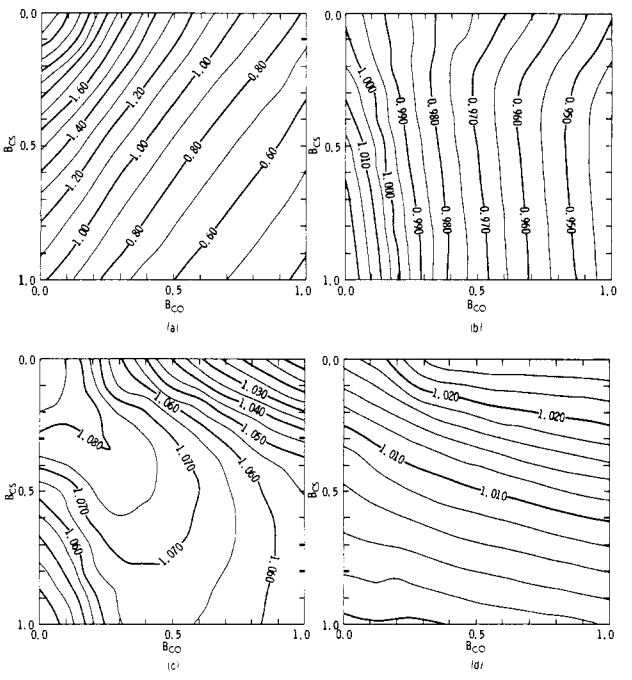

Figure 4. Isotopic maps for force-constant set no. 2 at 37 °C. The stretch–bend interaction has been included to produce a Walden-inversion reaction coordinate as in Figure 2. (a) Map of contours of constant $k(CH_3)/k(CD_3)$. (b) Map of contours of constant $k(^{16}O)/k(^{18}O)$. (c) Map of contours of constant $k(^{12}CH_3)/k(^{13}CH_3)$. (d) Map of contours of constant $k(^{32}S)/k(^{34}S)$.

Discussion

Validity of the Models. One point of comparison of the results of the present calculations with other experience is through the fractionation factors of Hartshorn and Shiner.[27] These are obtained by more careful vibrational analysis of stable molecules by the use of best-fit force fields rather than the simplified, estimated diagonal force fields we employed. From the Hartshorn–Shiner deuterium fractionation factors originally reported,[27]

(25) Available as supplementary material.
(26) Sampson, R. J. "Users' Manual for the Surface II Graphics System"; Technical Report, KOX Project, Kansas Geological Survey: Lawrence, KS, 1973.
(27) Hartshorn, S. R.; Shiner, V. J., Jr. *J. Am. Chem. Soc.* **1972**, *94*, 9002.

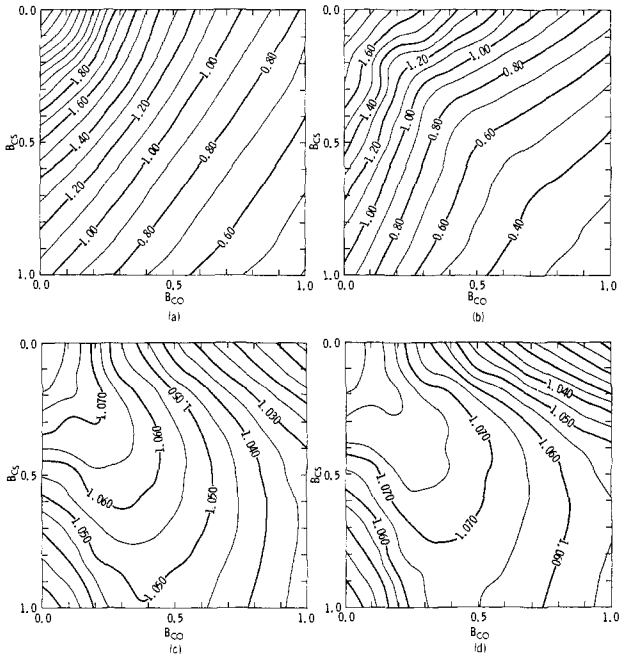

Figure 5. Maps similar to those of Figure 4, but in which various aspects have been altered to show their effects. (a) Map of $k(CH_3)/k(CD_3)$, to be compared with Figure 4a; the same force field is employed but the "rigid-methyl" reaction coordinate (eq 10 alone) is now imposed. The temperature is now 25 °C. Note that quantitative but not qualitative changes are introduced. (b) Another map of $k(CH_3)/k(CD_3)$, with the same "Walden-inversion" reaction coordinate as in Figure 4a, but with force-constant set no. 1. The temperature is 0 °C. (c) Map of $k(^{12}CH_3)/k(^{13}CH_3)$ with "rigid-methyl" reaction coordinate, force-constant set no. 2, temperature 25 °C; compare Figure 4c. (d) Map of $k(^{12}CH_3)/k(^{13}CH_3)$ with "Walden-inversion" reaction coordinate, force-constant set no. 1, temperature 25 °C, also to be compared to Figure 4c.

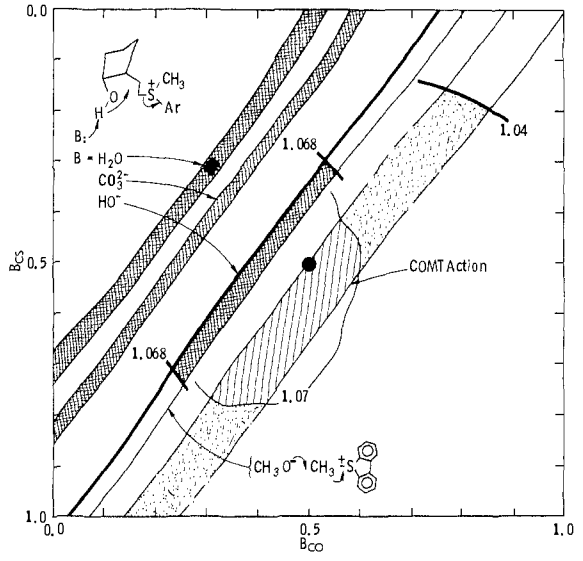

Figure 6. Isotopic map showing superposition of allowed-structure spaces for model and enzymic reactions. Starting from lower right, the first large diagonal space between the two light lines corresponds to $k(CH_3)/k(CD_3) = 0.83 \pm 0.05$ for COMT-catalyzed methylation of 3,4-dihydroxyacetophenone. The heavy lines crossing this space are the lower limits of $k(^{12}CH_3)/k(^{13}CH_3) = 1.09 \pm 0.02$ (calculated from the ratio of isotopic velocities, the latter independently averaged for a singly day) or 1.09 ± 0.05 (calculated from the ratios of velocities of adjacent isotopic runs, averaged over 3 days). The stippled and shaded spaces show the regions simultaneously consistent with both hydrogen and carbon isotope effects. The next space, proceeding "northwest", is for the α-deuterium effect of 0.97 ± 0.02 for the transmethylation reaction shown, limited by $k(^{12}CH_3)/k(^{13}CH_3) = 1.080 \pm 0.012$. The heavy black border is the allowed-structure space for the indicated cyclization reaction (HO^- catalysis), and the two remaining spaces are for CO_3^{2-} and H_2O catalysis, respectively. Only hydrogen isotope effects are available for the cyclization reaction. This map is based on those of Figure 4a,c.

one can interpolate or extrapolate to values[6] (relative to ethane) of 1.064 (DCH_2OR) and 1.026, 1.005, or 1.053 ($DCH_2SR_2^+$), depending in the latter case on the electrostatic correction used.[6] From these, the expected equilibrium isotope effect $K(CH_3)/K(CD_3)$ for the methyl transfer process of eq 1 is calculated as 0.84–0.97. We calculate equilibrium effects of 0.82 (force-constant set no. 1) or 0.76 (force-constant set no. 2). Because of the uncertainties connected with interpolation, extrapolation, and particularly electrostatic effects, the comparison is not unsatisfactory. It does suggest, however, that our force fields (particularly set no. 2) overestimate the inverse character of the deuterium isotope effects to be expected. A value for the equilibrium ^{13}C effect, $K(^{12}CH_3)/K(^{13}CH_3)$, can similarly be estimated[4] as 0.98. Our calculated values are 0.98 on both force-constant sets.

A second point of comparison is with experimental data. A collection[6] of 22 examples of $k(CH_3)/k(CD_3)$ for transmethylation reactions contains values from 0.87 to 1.13. Our calculated ranges at 298 K (the temperature dependence is small) are 0.35–1.67 (set no. 1, rigid-methyl reaction coordinate), 0.32–1.56 (set no. 1, Walden-inversion reaction coordinate), 0.49–2.29 (set no. 2, rigid-methyl reaction coordinate), 0.44–2.14 (set no. 2, Walden-inversion reaction coordinate). As the maps of Figures 4 and 5 show, the variation in magnitude is a nearly pure measure of "tight–loose" character of the transition state, the effects of about 0.3–0.5 (for 3D's) corresponding to extremely tight transition states ($B_{CS} + B_{CO} \rightarrow 2$) and effects of 1.16–1.32 per D corresponding to very loose, carbonium-like transition states ($B_{CS} + B_{CO} \rightarrow 0$). The observed experimental range thus falls entirely within the predicted limits and describes a relatively narrow band of structures. This is consistent with the view[6] that transmethylation (although not other transalkylation) transition states tend to be rather implastic in structure.

Thus the calculations yield effects in general agreement with expectations for equilibrium isotope effects and that encompass

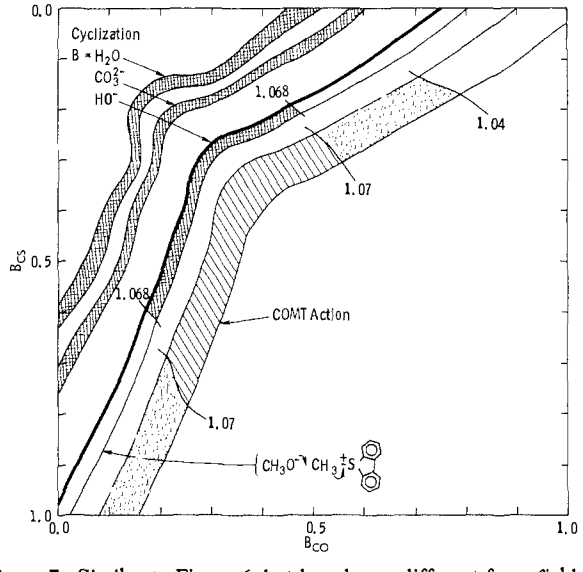

Figure 7. Similar to Figure 6, but based on a different force field; the basic maps are strongly similar to those of Figure 5a,c, but calculated for 37 °C.

all measured kinetic isotope effects, both for carbon and hydrogen isotopes. We conclude that they ought to give reliable conclusions, at least about relative structural features of related transition states and to some extent about absolute structures.

Transition-State Structures from Isotopic Maps. Figures 6 and 7 show maps upon which have been laid out the superposition of the regions encompassing structures "allowed" by hydrogen and carbon isotope effects for model and enzymic reactions. Figure 6 is drawn for the transition-state force field designated set no.

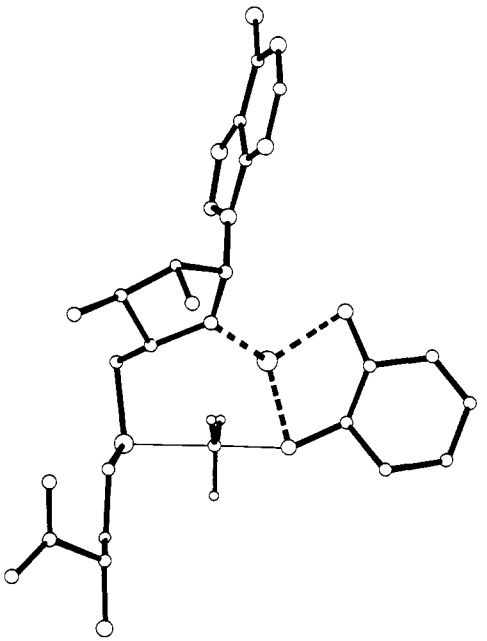

Figure 8. Possible transition-state structure for COMT-catalyzed methyl transfer. The structure corresponds to the heavy, circular mark in the center of Figure 6.

2, while Figure 7 is for the force field called set no. 1. Although the bond orders permitted by the different force fields for a particular transition state are not the same, the direction of change in transition-state structure, as reactions are changed, is the same in both cases. The discussion will be conducted in terms of Figure 6, and then the findings will be compared with results from Figure 7.

We begin with the region marked "COMT Action". The right-most diagonal line is a contour of constant isotope effect $k(CH_3)/k(CD_3) = 0.78$; this corresponds to the mean enzymic isotope effect[4] of 0.83 reduced by one standard deviation of 0.05. The next line above and to the left is a contour for $k(CH_3)/k(CD_3) = 0.88$ (i.e., 0.78 + 0.05). The region between these contains the combinations of B_{CS} and B_{CO} (roughly those for which $B_{CS} + B_{CO} \simeq 6.9-1.27$) that are allowed by the experimental α-deuterium isotope effect for the enzymic transition state. The lines accompanied by the numbers 1.04 and 1.07 serve to mark out the further limitations imposed by the carbon isotope effect. The mean value of $k(^{12}CH_3)/k(^{13}CH_3)$ for COMT action is 1.09; depending upon the method of data reduction, standard deviations from 0.02 to 0.05 may be estimated. Thus lines corresponding to two lower limits, 1.07 and 1.04, are shown. The upper limits lie beyond the calculated maximum. The most optimistic view is thus that the enzymic transition-state structure lies in the central, strongly shaded region ($B_{CS} \sim 0.2-0.6$, $B_{CO} \sim 0.3-0.6$, with only combinations having $B_{CS} + B_{CO} \sim 1.0-1.2$ permitted). A black, filled circle marks the "symmetrical" structure with $B_{CS} = B_{CO} = 0.5$. This structure should have a C–S bond length of about 2.0 Å and a C–O bond length of about 1.6 Å.

Both hydrogen and carbon isotope effects are also available for the nonenzymic reaction of methoxide ion with *S*-methyldibenzothiophenium ion. An allowed-structure space is traced out on the map for the transition state of this reaction.[28] Here the allowed structures have $B_{CS} \sim 0.3-0.7$, $B_{CO} \sim 0.25-0.6$, with $B_{CS} + B_{CO} \sim 0.9-1.0$. The most "symmetrical" structure ($B_{CS} = B_{CO} = 0.45$) would have C–S and C–O bond lengths around 0.03 Å longer than the corresponding lengths in the enzymic transition state.

(28) The carbon isotope effect of 1.080 ± 0.012, slightly different from our previous report[6] of 1.083 ± 0.015, derives from current work of Osborne Wong.

The cyclization model of Coward and his group,[5] depicted in the upper left of the map, has generated three α-deuterium effects (for the catalytic bases H_2O, CO_3^{2-}, and HO^-, as shown on the map) but as yet no carbon isotope effects. Even so, the results do suggest that the sum $B_{CS} + B_{CO}$ decreases from about 0.75–1.0 (HO^- catalysis) to 0.6–0.8 (CO_3^{2-} catalysis) to 0.5–0.7 (H_2O catalysis). The symmetrical structure for the "loosest" transition state is indicated by the black square at $B_{CO} = B_{CS} = 0.3$. This structure would have C–S and C–O bonds each longer by about 0.15 Å than those in the enzymic transition state.

The conclusions one would draw from a consideration of Figure 7 are not different in quality, but their numerical implications are different. This force field skews all symmetrical structures toward a "looser" region, but the ratio of bond orders for the lowest, symmetrical model-reaction transition state to those for the tightest enzymic transition state is 0.15/0.40 = 0.38, while the same ratio for the force field of Figure 6 is 0.40/0.65 = 0.62. The ratio of 0.38 corresponds to C–S and C–O bonds that are a maximum of 0.29 Å longer in the model-reaction transition state than in the enzymic transition state. The ratio of 0.62 corresponds to C–S and C–O bonds that are a maximum of 0.15 Å longer in the model-reaction transition state than in the enzymic transition state.

Catalytic Power and Transition-State Structure. The obvious conclusion from this treatment is in agreement with that from a more empirical approach involving the analysis of expected transition-state deuterium fractionation factors, which we reported before.[6] That is, the enzyme appears to *compress the S_N2 transition state*; it shortens the C–S and C–O bonds.

The present treatment casts this conclusion in somewhat more quantitative form. It suggests that the magnitude of this compression may well be of the order of 0.15 Å per bond and might conceivably be more than twice this amount. This is a large change in bond distance and ought to require a substantial expenditure of energy by the enzyme.

We have argued elsewhere[29] that the enzyme spends this compression energy in the transition state to alter the structure of the transition state so that it will resemble less strongly the preceding reactant molecules and the succeeding product molecules. Then the enzyme may *specifically* and strongly stabilize the transition state. Since the reactant and product species bear less resemblance than they otherwise would to this compressed structurally transformed transition state, the enzyme will "waste" less of its intrinsic binding energy in interactions with reactants and products. Further details of this concept, together with an energetic analysis, will be given elsewhere.

At this point, it is possible to construct a speculative model for the transition state, making use of the isotopic maps. Figure 8 shows a structure in which the C–S and C–O bond distances (2.0 and 1.6 Å, respectively) correspond to the heavy, black circular location in Figure 6. The two arms of the AdoMet molecule are shown arrayed about the transferring methyl in such a way that multipoint attraction at functional positions in these arms to positions in the enzyme structure can exert the force to compress the C–S bond. The dashed lines show possible coordinate linkages to the catalytically required magnesium(II) ion, suggesting a means for effecting the compression of the C–O bond. The energetic analysis and other work now in progress should test how valid this model is.

Acknowledgment. We are extremely grateful to Professor L. B. Sims for essential and generous help at many points. Dr. Ian Williams and Professors Gerald Maggiora and Marlin Harmony were also of constant aid in our work, and we thank them with pleasure.

Supplementary Material Available: Isotopic maps with explanatory notes (62 pages). Ordering information is given on any current masthead page.

(29) Olsen, J.; Wu, Y.-S.; Borchardt, R. T.; Schowen, R. L., in ref 2.